Available online at www.sciencedirect.com
SCIENCE DIRECT
Journal of Solid State Chemistry 179 (2006) 1339–1344
JOURNAL OF SOLID STATE CHEMISTRY
www.elsevier.com/locate/jssc

Compatibility evaluation between $La_2Mo_2O_9$ fast oxide-ion conductor and Ni-based materials

Gwenaël Corbel*, Philippe Lacorre

Laboratoire des Oxydes et Fluorures, UMR-6010 CNRS, Université du Maine, Avenue Olivier Messiaen, 72085 Le Mans Cedex 9, France

Received 6 December 2005; received in revised form 20 January 2006; accepted 22 January 2006
Available online 28 February 2006

Abstract

The chemical reactivity of $La_2NiO_{4+\delta}$ and nickel metal or nickel oxide with fast oxide-ion conductor $La_2Mo_2O_9$ is investigated in the annealing temperature range between 600 and 1000 °C, using room temperature X-ray powder diffraction. Within the $La_2NiO_{4+\delta}$/$La_2Mo_2O_9$ system, subsequent reaction is evidenced at relatively low annealing temperature (600 °C), with formation of La_2MoO_6 and NiO. The reaction is complete at 1000 °C. At reverse, no reaction occurs between Ni or NiO and $La_2Mo_2O_9$ up to 1000 °C. Together with a previous work [G. Corbel, S. Mestiri, P. Lacorre, Solid State Sci. 7 (2005) 1216], the current study shows that Ni-CGO cermets might be chemically and mechanically compatible anode materials to work with LAMOX electrolytes in solid oxide fuel cells.

Keywords: Lanthanum molybdate; K_2NiF_4-type structure; Chemical compatibility; Thermal expansion; Cathode; Nickel cermet anode; Electrolyte; SOFC

1. Introduction

In the field of solid oxide fuel cells, an active part of research focuses on finding better electrolytes than yttria stabilized zirconia (YSZ) the state-of-the-art material in the field. One of the main purposes is to lower working temperature, which should lessen risks of reactivity with electrode materials. A few years ago, our team has discovered a new family of fast oxide-ion conductors, the so-called LAMOX family, whose parent compound is lanthanum molybdate $La_2Mo_2O_9$ [1–3]. This oxide exhibits, above 600 °C, a higher oxide-ion conductivity than YSZ8%, the best stabilized zirconia, which should result in a decrease of working temperature by more than 150 °C. A stabilization of this molybdate against phase transition and reducibility is achieved through appropriate substitution, particularly of molybdenum by tungsten [4,5].

In a recent paper, we have started studying the compatibility of $La_2Mo_2O_9$ with typical electrode materials for solid oxide fuel cells, such as $La_{0.6}Sr_{0.4}Co_{0.2}Fe_{0.8}O_{3-\delta}$ (LSCF), $La_{0.8}Sr_{0.2}MnO_{3-\delta}$ (LSM) and $Ce_{0.9}Gd_{0.1}O_{1.95}$ (CGO) [6]. If LSCF and LSM start reacting with the molybdate above 700–800 °C (typically through strontium migration from one phase to the other), CGO does not react up to 1000 °C. In the current paper, we are now studying the reactivity/compatibility of $La_2Mo_2O_9$ with the nickel-based materials $La_2NiO_{4+\delta}$ and Ni. $La_2NiO_{4+\delta}$ is considered to be a good cathode material, especially in terms of both ionic conductivity and electrocatalytic properties [7]. Nickel, on the other side, is commonly used at the anode in combination with usual electrolytes (YSZ or CGO, for instance) in so-called cermets prepared from a mixture with NiO, then reduced to metallic nickel. Note that zirconia should be avoided with LAMOX since it tends to react to form the parasitic insulating $La_2Zr_2O_7$ phase, as we showed earlier [8]. CGO however is unreactive, as mentioned above.

Here we use room temperature X-ray powder diffraction to study the materials chemical compatibility from annealings, at various temperatures, of equimolar mixtures $La_2Mo_2O_9$/$La_2NiO_{4+\delta}$ and $La_2Mo_2O_9$/Ni.

*Corresponding author. Laboratoire des Oxydes et Fluorures, UMR-6010 CNRS, Institut de Recherche en Ingénierie Moléculaire et Matériaux Fonctionnels, IRIM2F, FR CNRS 2575, Université du Maine, Avenue Olivier Messiaen, 72085 Le Mans Cedex 9, France.
Fax: +33 02 43 83 35 06.
E-mail address: gwenael.corbel@univ-lemans.fr (G. Corbel).

0022-4596/$ - see front matter © 2006 Elsevier Inc. All rights reserved.
doi:10.1016/j.jssc.2006.01.051

Thermodiffractometry is also used to check for thermal expansion coefficients compatibility.

2. Experimental details

Polycrystalline α-$La_2Mo_2O_9$ was prepared by conventional solid-state reaction. The stoichiometric mixture of La_2O_3 and MoO_3 was first heated at 500 °C for 12 h, and then at 900 °C with several regrindings and heatings. Prior to use, La_2O_3 was calcinated in air during 12 h at 1000 °C in order to remove adsorbed water and carbon dioxide.

A 5 g polycrystalline sample of $La_2NiO_{4+\delta}$ was synthesized from a fine and intimate mixture of oxides obtained from the thermal decomposition of the corresponding nitrates. The nitrates were prepared by dissolution of a stoichiometric quantities of La_2O_3 and Ni powders in a nitric acid solution (65%, Fischer Scientific) and by slowly evaporating the excess of acid up to 150 °C on a hot plate. The decomposition of the green residue, spread over the bottom of an alumina boat, was carried out in an argon flow at 500 °C (2 h, heating rate 2 °C/min). This intimate mixture of oxides was then fired 12 h at 900 °C in argon. The resulting powder was then heated in air for 72 h at 1250 °C (heating and cooling rates 5 °C/min) with intermediate grindings into acetone. Finally, a low temperature annealing in pure oxygen (1 atm) at 450 °C for 12 h with slow cooling down to room temperature was performed. The resulting sample was dark brown to black in color. The overall oxygen stoichiometry was determined by reduction in a diluted hydrogen flow (6%H_2 and 94%N_2) at 800 °C (heating rate 0.5 °C/min) of ~50.1 mg performed with a TGA/DSC Q600 SDT TA Instuments apparatus. Alumina powder was used as a reference.

For the reactivity studies, equimolar amounts of $La_2NiO_{4+\delta}$ or Ni and α-$La_2Mo_2O_9$, thoroughly ground in an agate mortar, were spread in an alumina boat. To follow the reactivity evolution, the mixtures were fired in air for 72 h at five arbitrary temperatures 600, 700, 800, 900 and 1000 °C (heating and cooling rates 2 °C/min). After completion, X-ray powder diffraction patterns were recorded at room temperature on a θ/θ Bragg-Brentano Philips X'pert MPD PRO diffractometer (Cu$K\alpha_{1+2}$ radiations) equipped with the X'celerator detector. The annealed powder was dusted through a 63 μm sieve on a glass holder. Diffractograms were collected at room temperature during 400 min in the [5–130°] scattering angle range, with a 0.0084° step. The Rietveld program FullProf [9] was used for full-pattern matching and/or Rietveld refinements. Thermodiffractograms were recorded on the same diffractometer equipped with a HTK 1200 Anton Paar chamber. Diffractograms of NiO were collected under air flow during 230 min in the [35–130°] scattering angle range, with a 0.0084° step from 25 to 1060 °C (heating rate 10 °C/min, temperature stabilization for 20 min with temperature correction after calibration [6]).

3. Results and discussion

The starting materials $La_2NiO_{4+\delta}$ and α-$La_2Mo_2O_9$ were first analyzed by X-ray powder diffraction in order to determine their cell parameters and check their purity. All oxides were monophasic.

At room temperature, $La_2NiO_{4+\delta}$ exhibits an orthorhombic distortion of the ideal tetragonal K_2NiF_4-type structure [10]. Whole pattern matching refinements were then carried out in the *Fmmm* (no. 69) space group and lead to cell parameter values $a = 5.4597(1)$ Å, $b = 5.4656(1)$ Å, $c = 12.6900(1)$ Å and $V = 378.67(1)$ Å in good agreement with the literature data. Weight loss curve associated to the reduction of $La_2NiO_{4+\delta}$ in a diluted hydrogen flow shows two broad plateaus (490–560 and 670–800 °C) corresponding to a two-steps reduction (Fig. 1). In a first stage, the oxide was reduced into stoichiometric $La_2NiO_{4.00}$ (0.60% weight loss) and then into lanthanum sesquioxide and nickel metal (3.88% weight loss). The endothermic peak recorded at 625 °C is associated to the decomposition of lanthanum nickelate to La_2O_3 and Ni, clearly identified by X-ray powder diffraction. The reaction of the reduction-decomposition can be written as follows:

$$La_2NiO_{4+\delta} + (1+\delta)H_2 \rightarrow La_2O_3 + Ni + (1+\delta)H_2O.$$

The weight loss allowed to determine the oxygen overstoichiometry $\delta = 0.13$ of the oxygen-annealed sample.

At room temperature, α-$La_2Mo_2O_9$ exhibits a slight monoclinic distortion and a $2 \times 3 \times 4$ superstructure relative to the cubic β form [2]. A good pattern matching fit ($\chi^2 = 2.76$, R Bragg = 2.96%) can be obtained in a single monoclinic subcell $a = 7.1414(1)$ Å, $b = 7.1538(1)$ Å, $c = 7.1653(1)$ Å, $\beta = 89.530(1)°$ and $V = 366.05(1)$ Å using the space group $P2_1$ (no. 4) and neglecting the superstructure peaks at low 2θ scattering angle. All unit cell parameters were used as starting values for the fitting procedure of the X-ray diffraction patterns of annealed mixtures.

3.1. The $La_2NiO_{4+\delta}$/α-$La_2Mo_2O_9$ system

For this system, the room temperature X-ray diffraction patterns clearly show, after firing at temperatures above 600 °C, the appearance of an La_2MoO_6 type phase [11] (Fig. 2). For the mixture annealed at 600 °C, the proportion is rather small as only one weak diffraction line (103) associated to La_2MoO_6 was observed (not visible to the naked eye in Fig. 2a). Finally, above 900 °C, extra diffraction lines were detected and attributed to an additional phase NiO (rhombohedral distortion of the cubic rock-salt structure) (Fig. 2b).

As a consequence, the presence of the extra phases were taken into account in Rietveld refinements of diffraction patterns. Note that only α-$La_2Mo_2O_9$ is treated in full-pattern matching mode because of the complexity of its structure [3]. From these refinements, molar percentages of

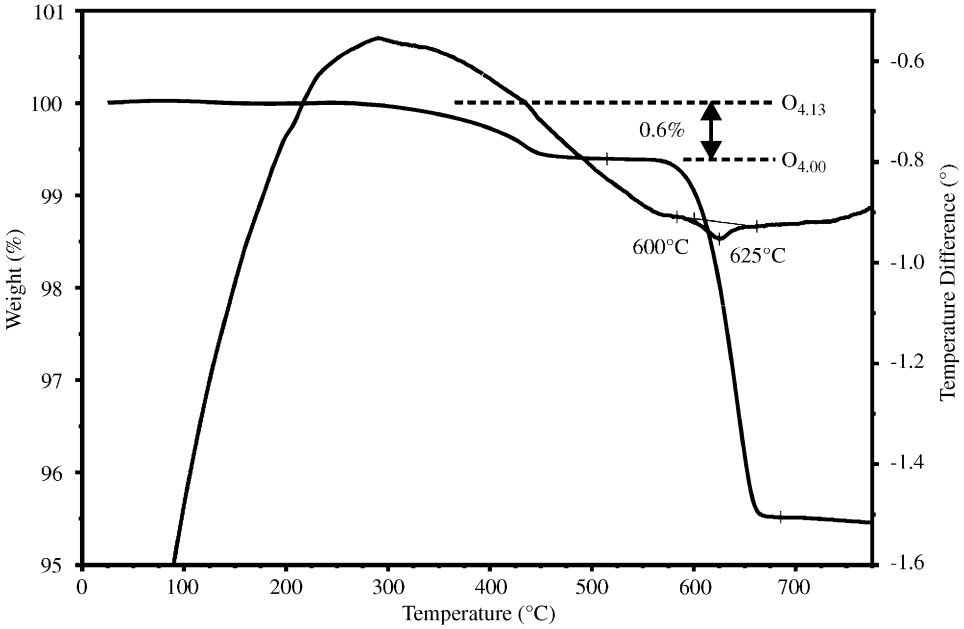

Fig. 1. DTA–TGA curves of the oxygen-annealed sample of $La_2NiO_{4+\delta}$.

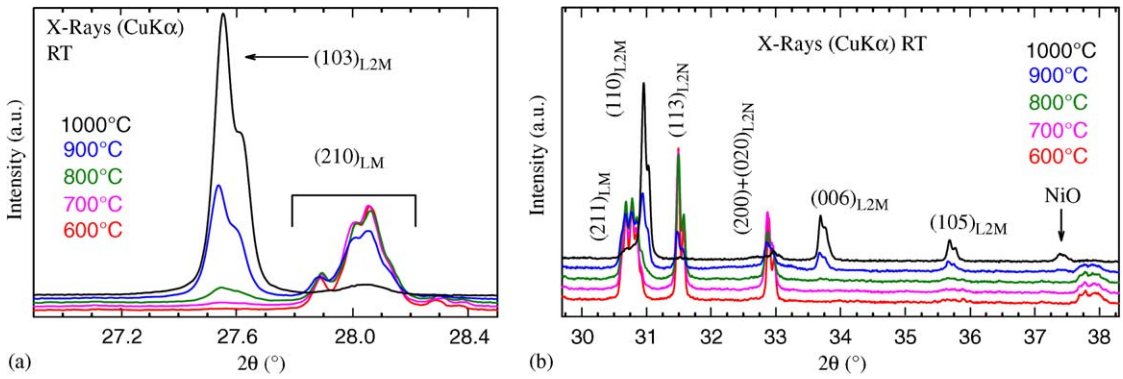

Fig. 2. Selected areas of the X-ray diffraction patterns of $La_2NiO_{4+\delta}$/α-$La_2Mo_2O_9$ (L2N/LM) mixture after annealing at different temperatures. The La_2MoO_6 phase is noted L2M. For LM, indices are given in the single monoclinic cell.

$La_2NiO_{4+\delta}$, La_2MoO_6 and NiO were determined and plotted as a function of annealing temperature in Fig. 3. The cell volume evolutions of $La_2NiO_{4+\delta}$, α-$La_2Mo_2O_9$, La_2MoO_6 and NiO oxides with the annealing temperatures are presented in Fig. 4. It must also be noted that, in the whole range of annealing temperature explored, the pseudo-cubic (210) (Fig. 2a) and (123) peak splittings characteristic of the slight monoclinic distortion in α-$La_2Mo_2O_9$ remain unchanged, contrary to what was observed in the reactions with LSM and LSCF [6].

From these tests, a reaction between the oxides $La_2NiO_{4+\delta}$ (L2N) and α-$La_2Mo_2O_9$ (LM) is clearly evidenced at relatively low annealing temperature. Lanthanum nickelate could be considered as lanthanum sesquioxide source in the formation of La_2MoO_6 (L2M) from α-$La_2Mo_2O_9$ (doubling of La/Mo molar ratio). No crystal cell evolution is noted for reactants and reaction products (see Figs. 2 and 4). Furthermore, raw powders of $La_2NiO_{4+\delta}$, fired in air for 72 h at 600,700, 800, 900 and 1000 °C (open triangles in Fig. 4), show identical cell volumes as those observed in the L2N/LM system. Consequently, the reaction occurring within the L2N/LM system does not arise from a slow lanthanum depletion from lanthanum nickelate ($La_{2-x}NiO_{4+\delta}$) as the annealing temperature increases. Similarly, no change is observed in the α-$La_2Mo_2O_9$ diffraction pattern. Therefore no solid solution resulting from species migration from one phase to the other is observed, and the process has to be considered as a decomposition–recombination reaction. The reaction is considerably accelerated above 800 °C, as three quarter of lanthanum nickelate is already consumed at 900 °C (Fig. 3). At a high decomposition rate of the lanthanum nickelate, above 800 °C, NiO with fewer diffracting electrons can be detected by X-ray powder diffraction. Finally, lanthanum nickelate has totally disappeared after the annealing at 1000 °C. The fact that

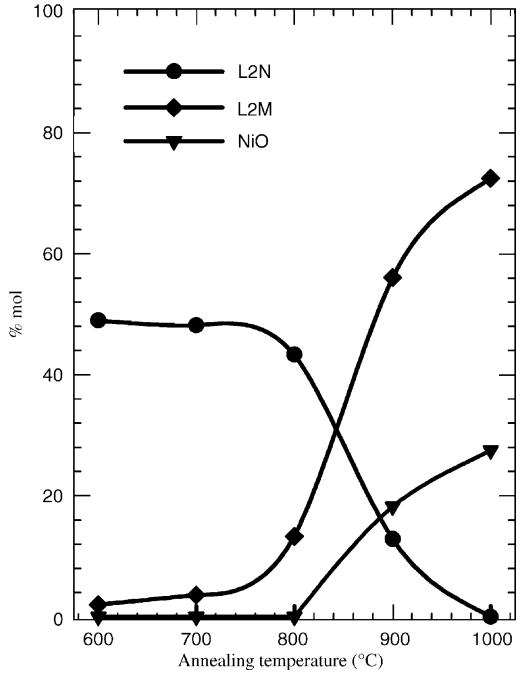

Fig. 3. Annealing temperature dependence of molar proportions of $La_2NiO_{4+\delta}$ (L2N), La_2MoO_6 (L2M) and NiO in the reaction of $La_2NiO_{4+\delta}$ with $La_2Mo_2O_9$ (assuming a mole per mole reaction).

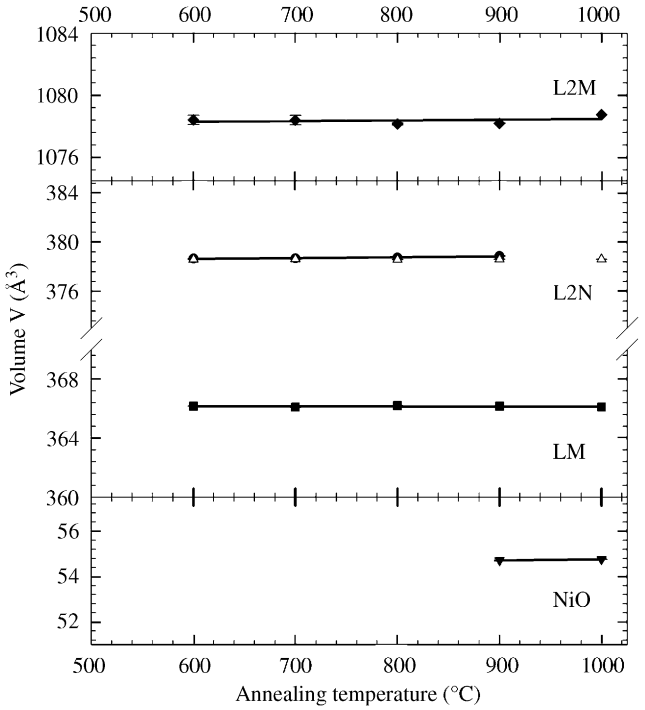

Fig. 4. Variations of the unit cell volume of La_2MoO_6 (L2M), $La_2NiO_{4+\delta}$ (L2N), α-$La_2Mo_2O_9$ (LM, single monoclinic) and NiO as a function of the mixture's annealing temperature. Open triangles are relative to the annealing of raw $La_2NiO_{4+\delta}$ powders. Error bars are approximately the size of the data points.

no diffraction peak relative to nickel oxide is observed below 900 °C, cannot be ascribed to any nickel diffusion into α-$La_2Mo_2O_9$ as no cell volume variation or stabilization of β type phase is noted. This is corroborated by the failure to prepare any nickel substituted lanthanum molybdate $La_2Mo_{2-y}Ni_yO_{9-\delta}$ by solid-state reaction, the resulting products being α-$La_2Mo_2O_9$, La_2MoO_6 and NiO. The decomposition-recombination reaction can be written as follows:

$$La_2NiO_{4+\delta} + \alpha\text{-}La_2Mo_2O_9 \rightarrow 2La_2MoO_6 + NiO + \delta/2O_2.$$

The molar ratio 2:1 given by this reaction is in fair agreement with the molar proportions of 72% and 28% determined from Rietveld refinements for La_2MoO_6 and NiO, respectively (Fig. 3), after annealing at 1000 °C.

3.2. The Ni/α-$La_2Mo_2O_9$ system

In this system, after annealing below 700 °C, small amount of nickel remains present, but most Ni has been oxidized to NiO, oxidation being complete at higher temperature as confirmed by the light green color of the powder. All X-ray diffractograms were fully indexed as α-$La_2Mo_2O_9$ and NiO phases, no subsidiary phases were found and no stabilization of the cubic form of $La_2Mo_2O_9$ was observed (inset Fig. 5). At room temperature, nickel oxide adopts a rhombohedral distorsion of the cubic rock-salt structure. Then cell parameters refinements were performed using space group $R\bar{3}m$ (no. 166) in the hexagonal description. A typical whole pattern fitting of X-ray powder diffraction diagram is presented in Fig. 5. As can be seen in Fig. 6, no cell volume evolution is observed for both materials. A good chemical compatibility between Ni or NiO and lanthanum molybdate is then clearly demonstrated.

The thermal expansion coefficient (TEC) of nickel oxide was estimated from the temperature dependence of unit cell parameters obtained by full-pattern matching refinements of X-ray thermodiffractograms. Nickel oxide undergoes a rhombohedral ($R\bar{3}m$)-antiferromagnetic→cubic ($Fm\bar{3}m$)-paramagnetic magnetostrictive transition around 190 °C. The trigonal distortion at low temperature is accompanied by a small contraction of the unit cell along the 3-fold axis, detectable on X-ray thermodiffractograms. Two TEC values were determined from linear regressions applied above and below this transition: $14.4 \times 10^{-6}\,°C^{-1}$ (RT-190 °C) and $15.7 \times 10^{-6}\,°C^{-1}$ (190–1060 °C). The average value is slightly larger than the coefficients of $14.1 \times 10^{-6}\,°C^{-1}$ [12] and $14.2 \times 10^{-6}\,°C^{-1}$ [13] determined by dilatometry measurements and reported in the literature. It is interesting to note that the TEC value of nickel metal, $16.9 \times 10^{-6}\,°C^{-1}$ [12], is larger than that of NiO and CGO ($11.9 \times 10^{-6}\,°C^{-1}$) [6]. A comparative graph of thermal expansion of LM, CGO, Ni and NiO is shown in Fig. 7. The use of nickel in cermet anode based on CGO would reduce the difference of TECs between $La_2Mo_2O_9$ ($15.7–20.1 \times 10^{-6}\,°C^{-1}$, RT-1060 °C) [6] and CGO. A closer thermal expansion match could also be expected

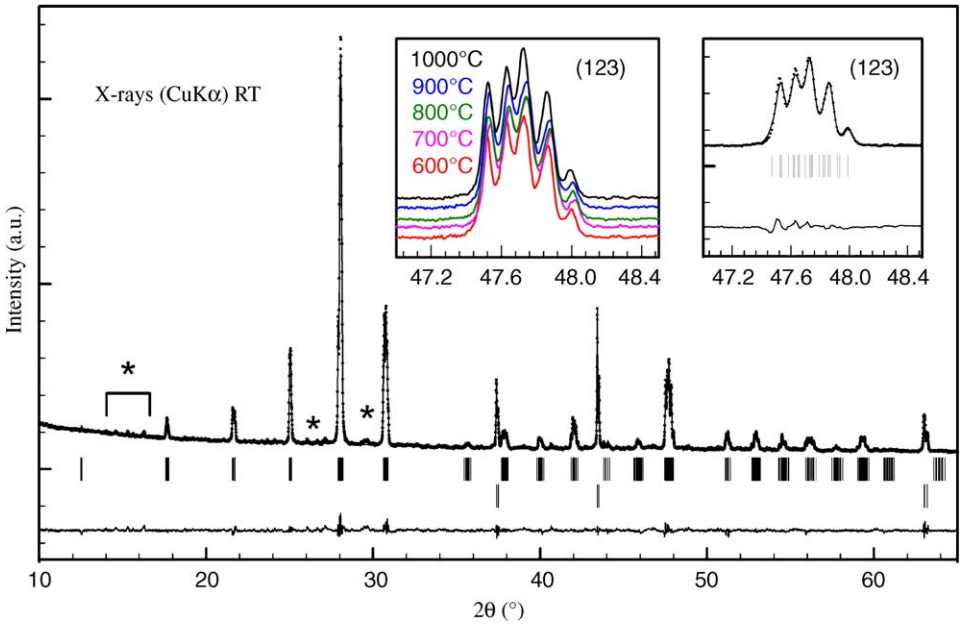

Fig. 5. Full-pattern matching (observed = dots, calculated = lines, difference below) of the X-ray diffraction patterns of an Ni/α-$La_2Mo_2O_9$ mixture after annealing 72 h in air at 1000 °C. The first and second rows in the reflection lines correspond to α-$La_2Mo_2O_9$ (asterisks indicate the superstructure reflections) and NiO, respectively. In inset: detail showing the invariance with annealing temperature of the splitting of the (123) pseudo-cubic reflection line (Cu$K\alpha_{1+2}$ wavelength) of α-$La_2Mo_2O_9$.

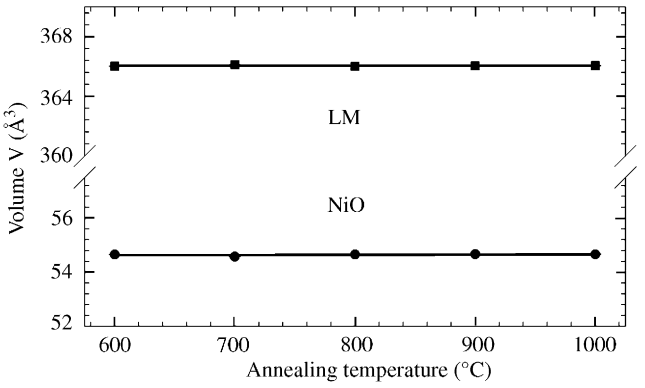

Fig. 6. Absence of variation of the unit cell volume of NiO (hexagonal description) and of α-$La_2Mo_2O_9$ (LM, single monoclinic) as a function of the mixture's annealing temperature. Error bars are approximately the size of the data points.

by combining appropriate chemical substitutions of lanthanum or/and molybdenum.

4. Conclusion

We have shown that a significant reactivity exists between the oxides $La_2NiO_{4+\delta}$ and α-$La_2Mo_2O_9$ even at relatively low annealing temperature (600 °C), precluding the use of both types of materials together in solid oxide fuel cells. LSM appears at the moment the less reactive cathode material tested up to now [6], but chemical compatibility still has to be improved at this side. At reverse, no reaction is observed between Ni or NiO and $La_2Mo_2O_9$ even up to 1000 °C. This is to be paralleled with the absence of any reaction between CGO and $La_2Mo_2O_9$

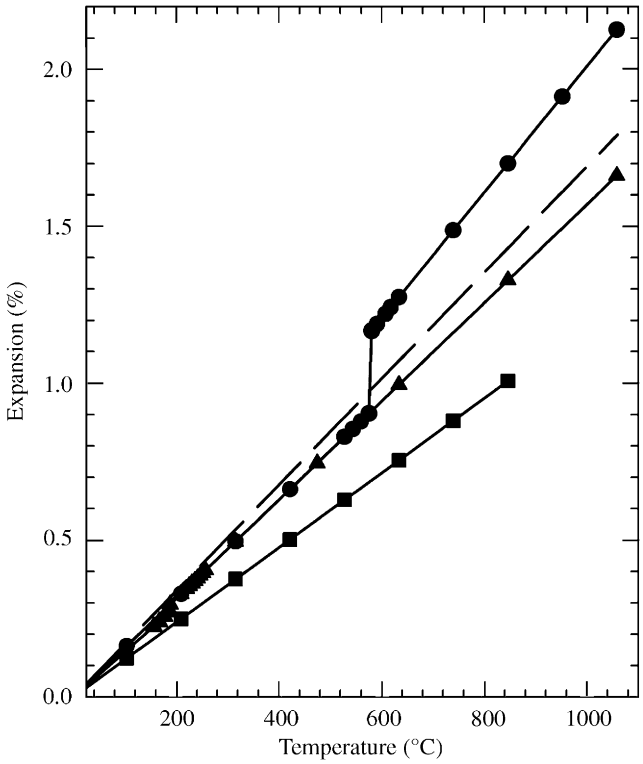

Fig. 7. Thermal expansion of $La_2Mo_2O_9$ (circles, from [6]), $Ce_{0.9}Gd_{0.1}O_{1.95}$ (squares, from [6]), NiO (triangles) and Ni (dashed line, from [12]) in air.

[6], which make Ni–CGO cermets with comparable thermal expansion coefficients potentially interesting anode materials for LAMOX electrolytes. If Ni–$La_2Mo_2O_9$ cermets seem to be banned due to the reducibility of $La_2Mo_2O_9$

[14], a cermet Ni-LAMOX with more stable tungsten substituted $La_2Mo_2O_9$ [4] might also be investigated.

References

[1] P. Lacorre, F. Goutenoire, O. Bohnke, R. Retoux, Y. Laligant, Nature 404 (2000) 856.
[2] F. Goutenoire, O. Isnard, R. Retoux, P. Lacorre, Chem. Mater. 12 (2000) 2575.
[3] I.R. Evans, J.A.K. Howard, J.S.O. Evans, Chem. Mater. 17 (2005) 4074.
[4] S. Georges, F. Goutenoire, Y. Laligant, P. Lacorre, J. Mater. Chem. 13 (2003) 2317.
[5] D. Marrero-López, J. Canales-Vásquez, J.C. Ruiz-Morales, J.T.S. Irvine, P. Núñez, Electrochim. Acta 50 (2005) 4385.
[6] G. Corbel, S. Mestiri, P. Lacorre, Solid State Sci. 7 (2005) 1216.
[7] S.J. Skinner, J.A. Kilner, Solid State Ionics 135 (2000) 709.
[8] S. Georges, F. Goutenoire, P. Lacorre, M.C. Steil, J. Eur. Ceram. Soc. 25 (2005) 3619.
[9] J. Rodriguez-Carvajal, Physica (Amsterdam) 192B (1993) 55.
[10] J.D. Jorgensen, B. Dabrowski, S. Pei, D.R. Richards, D.G. Hinks, Phys. Rev. B 40 (4) (1989) 2187.
[11] J.S. Xue, M.R. Antonio, L. Soderholm, Chem. Mater. 7 (1995) 333.
[12] M. Mori, T. Yamamoto, H. Itoh, H. Inaba, H. Tagawa, J. Electrochem. Soc. 145 (4) (1998) 1374.
[13] Thermophysical Properties of Matter, The TPRC Data Series Vol. 13, Thermal Expansion, Nonmetallic Solids, 1977.
[14] F. Goutenoire, R. Retoux, E. Suard, P. Lacorre, J. Solid State Chem. 142 (1999) 228.